Research Article

A Simulation of *H*-mode Plasma in DIII-D Tokamak with Complete Core-Edge-SOL Model Using Integrated Predictive Modeling Code

Yutthapong Pianroj*, Saysunee Jumrat and Warit Werapun
Faculty of Sciences and Industrial Technology, Prince of Songkla University
Surat Thani Campus, Surat-Thani 84000, Thailand

Thawatchai Onjun
School of Manufacturing System and Mechanical Engineering,
Sirindhorn International Institute of Technology, Thammasat University
Rangsit Campus, Khlong Nueng, Klong Luang, Pathum Thani 12120, Thailand

Abstract

A prediction model of *H*-mode tokamak plasmas including scrape-off layer (SOL) is investigated, developed and tested in the integrated predictive modeling code named BALDUR. The SOL region is calculated by the two chamber model. Then the formation of the pedestal, a narrow edge plasma region, where a pressure gradient is formed, is calculated by a semi-empirical anomalous core transport model named Mixed Bohm/gyro-Bohm (Mixed B/gB) and the Chang-Hinton neoclassical transport models, which are extended to be applicable for this region by the suppression due to the $\omega_{E\times B}$ flow shear and magnetic shear effects. Because of the reduction of transport in the outer region of the plasma, the pedestal can be formed and evolved. The last region is the plasma core, in which a fusion reaction takes place. The plasma core is calculated by a modified semi-empirical anomalous core transport model Mixed B/gB. This full prediction model is used to simulate the time evolution of plasma current, ion and electron temperature, and electron and ion density profiles for 10 DIII-D *H*-mode discharges. It is found that the *H*-mode plasma profiles can be seen in all BALDUR simulations. Root-mean-square errors (RMSE) and offsets are calculated to quantify the agreement with the simulated pedestal formation profiles and those obtained from experiment.

Keywords: *H*-mode plasma; tokamak plasma; SOL; pedestal and integrated predictive modeling code

1. Introduction

The High Confinement mode (*H*-mode) is an important regime for burning plasma experiments using the magnetic confinement fusion concept because it provides high temperature and excellent energy confinement time. Many experiments, such as Doublet III-Device (DIII-D), Joint European Torus (JET), and Tokamak Fusion Test Reactor (TFTR), have decided to operate

***Correspondence** : yutthapong.p@psu.ac.th DOI 10.14456/tijsat.2016.13

the tokamaks in this regime, ITER (International Thermonuclear Experimental Reactor) will also be operating in this regime [1]. Normally, the tokamak plasma can be divided into three main regions, shown in Figure 1 [2].

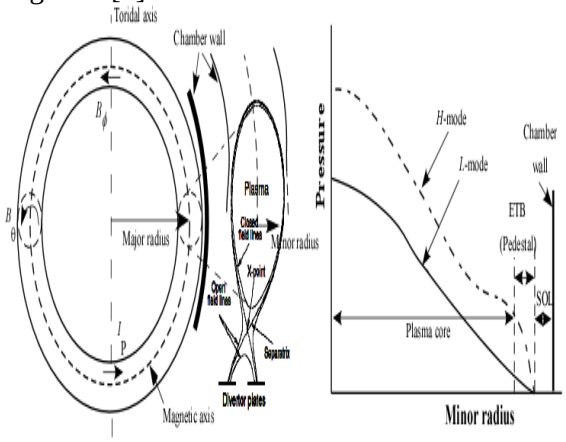

Figure 1. A geometric sketch of tokamak illustrates the technical terms used in the text. The major radius is measured from the toroidal axis to the geometric center of the plasma, while the minor radius is measured from the geometric center to the edge of the plasma. The magnetic field consists of two components: a toroidal magnetic field B_ϕ, and a poloidal magnetic field.B_θ The graph on the right shows the pressure profiles along the minor radius, for *L*-mode and *H*-mode operations. The three main regions of tokamak plasma: plasma core, edge (pedestal), and SOL, are indicated.

The core plasma region extends from the center of the plasma up to the edge region that is close to separatrix. In this region, the plasma is confined then it is produced the fusion energy from this zone. The edge plasma region is a narrow region which is located between the core region and the separatrix. Normally, at this region the transport barrier will be present in *H*-mode plasma. The edge transport barrier (ETB) is characterized by sharp temperature and density gradients named "pedestal". However, when tokamak plasma is operated in *L*-mode, the pedestal does not form because the total power is lower than the threshold power [3]. The Scrape-off-Layer (SOL) is the region outside of the last closed magnetic flux surface or separatrix, where magnetic field lines run into the limiter or divertor. The SOL plasma is essentially governed by two-dimensional effects, such as the flows of heat and particles along magnetic field lines as well as across field lines. The physics of the SOL is dominated by atomic process and plasma wall interactions. This physics is obtained by the particle flow to material surfaces; it is primarily due to diffusion from the plasma core into the edge region. In the edge boundary layer the plasma flows along the magnetic field and then interacts with a solid surface. Ions which are incident at this surface may then be neutralized and backscattered or released in other ways to re-enter the plasma. This process is known as "*recycling*".

Therefore, the importance of SOL is illustrated as its function as a "*sink and source"* of energy and particles for tokamak plasma. The particle and heat-loss model at the SOL that has been developed by W. D. Langer and C. E. Singer [4] is used to predict the plasma profiles in SOL region then the plasma profiles are evolved to edge and core region with Mixed Bohm and gyroBohm (Mixed B/gB) transport model to compare with the experiments that concentrate on systematic scans of *H*-mode discharges in the Doublet III Device (DIII-D) tokamak. This work is organized as follows: the details of an SOL model will be described in the next section, followed by information about the anomalous core transport Mixed B/gB and the pedestal formation model. In section 3, the simulation results for standard *H*-mode will be validated by the statistical method compared to the experimental data from tokamak DIII-D; they are presented and discussed. The final section is the conclusion.

Simulation Model and Descriptions Two Chambers Model

Plasma transport models of radial flow in tokamaks with a divertor or pumped limiter must include particle and heat-loss terms due to flow along magnetic-field lines in the scrape-off. The plasma entering the scrape-off flows along open field lines until it reaches the neutralizer plate. The resulting neutral gas interacts with the incoming plasma and modifies its properties and flow. The greatest effect occurs when there is a large recycling of the neutral gas. This happens when the neutrals are ionized by the plasma near the neutralizer and are swept back to the neutralizer with the cycle repeated a number of times. This enhancement of the plasma flow near the neutralizing surface serves to amplify the particle flux and reduce the temperature, thereby minimizing erosion. The amplification of particle flux due to recycling also reduces the upstream plasma flow velocity along the field lines in the scrape-off, thus changing the edge density of the main plasma region. To solve for the flow of material entering the scrape-off into a high-recycling region, the model ignores all radial flows in the scrape-off and considers only parallel flow along the field lines. The fluid equations, including sources, have been derived in arbitrary coordinates. When cross-field transport near the mid-plane is sufficient to give broad profiles of density and temperature, only flow along the field lines needs be considered near the divertor. Assuming a constant ratio of poloidal to total magnetic field B_θ/B, the fluid equation for the flow of ions, total momentum, and total energy can be written as Equations 1-3, respectively:

$$\frac{d}{ds}(nu) = S_i \tag{1}$$

$$\frac{d}{ds}\left(mnu^2 + n(T_e + T_i)\right) = 0 \tag{2}$$

$$\frac{d}{ds}\left[q^e + \left(\frac{5}{2}n(T_e + T_i) + \frac{1}{2}mnu^2\right)u\right] = W \tag{3}$$

where s is a distance along the magnetic-field line, n is a fluid density, u is a fluid velocity, m is an ion mass, S_i is an ion source due to ionization of neutrals, W is an energy source, q^e is a parallel electron heat conduction, and T_e and T_i are electron and ion temperature, respectively.

MIXED BOHM/GYRO-BOHM (Mixed b/gB) Model

The Mixed B/gB model is a semi-empirical anomalous core transport model which consists of a combination of Bohm and gyro-Bohm scaling. For the Bohm scaling, it is proportional to the gyro-radius times thermal velocity over a plasma linear dimension such as major radius. Transport diffusivities of this scaling are functions of the profile shapes which are characterized by normalized gradients and a magnetic safety factor q which are assumed to be held fixed in systematic scans in which only the gyro-radius is changed relative to plasma dimensions. For the gyro-Bohm scaling, the transport diffusivities are proportional to the square of the gyroradius times thermal velocity over the square of the plasma linear dimension, so the Mixed B/gB transport model can be expressed as Equation 4-7[5]:

$$\chi_{\mathrm{e}} = 1.0\chi_{\mathrm{gB}} + 2.0\chi_{\mathrm{B}} \tag{4}$$

$$\chi_{\mathrm{i}} = 0.5\chi_{\mathrm{gB}} + 4.0\chi_{\mathrm{B}} + \chi_{\mathrm{neo}} \tag{5}$$

$$\mathrm{D_H} = [0.3 + 0.7\rho]\frac{\chi_{\mathrm{e}}\chi_{\mathrm{i}}}{\chi_{\mathrm{e}}+\chi_{\mathrm{i}}} \tag{6}$$

$$D_z = [0.3 + 0.7\rho]\frac{\chi_{\mathrm{e}}\chi_{\mathrm{i}}}{\chi_{\mathrm{e}}+\chi_{\mathrm{i}}} \tag{7}$$

where,

$$\chi_{\mathrm{gB}} = 5 \times 10^{-6}\sqrt{\mathrm{T_e}}\left|\frac{\nabla \mathrm{T_e}}{\mathrm{B_\phi^2}}\right| \tag{8}$$

$$\chi_{\mathrm{B}} = 4 \times 10^{-5} R \left|\frac{\nabla(n_{\mathrm{e}}\mathrm{T_e})}{n_{\mathrm{e}}B_\phi}\right| q^2 \left(\frac{T_{\mathrm{e},0.8} - T_{\mathrm{e},1.0}}{T_{\mathrm{e},1.0}}\right) \tag{9}$$

where, χ_{e} is the electron diffusivity, χ_{i} is the ion diffusivity, D_H is the particle diffusivity, $\mathrm{D_z}$ is the impurity diffusivity, χ_{gB} is the gyro-Bohm contribution, χ_{B} is Bohm contribution, T_{e} is the electron temperature in keV, B_ϕ is the toroidal magnetic field, R is the major radius, n_{e} is the

local electron density, q is the safety factor, and s is the magnetic shear. In this work, the effect of ELMs is not included. As a result, the results are obtained at the peak value of the pedestal before ELMs occur.

Pedestal Formation Model

The major purpose of modelling the edge transport is to understand and predict the formation of the pedestal structure such as the variation of the pedestal width and height for the plasma density and temperature. The pedestal structure evolves on a transport time scale, but during this evolution, magnetohydrodynamic (MHD) phenomena with very short time scales occur, as from type-I edge localized modes (ELMs) [6]. The occurrence of an ELM burst produces a significant pulsed flow of particles and energy onto the divertor target, diminishing the edge pressure gradients in the process. Thus, the modelling of the transport barrier width is not yet well developed. An appropriate transport suppression function (f_s) due to $\omega_{E\times B}$ flow shearing rate together with the reduction of turbulence growth rate [7-9] is represented in the first term which the $\vec{E} \times \vec{B}$ flow shear alone produces pedestals which are appreciably lower than those experimentally obtained. Therefore, an additional magnetic shear stabilization is included in the second term [10-11]. The transport is reduced only in the region where the magnetic shear exceeds the threshold (in this work the threshold is 0.5 [11]) and the suppression function can be shown in Equation 10. Moreover, we assume all the simulations evolved the temperature pedestal width and height during the ELM-free phase.

$$f_{s_x} = \frac{1}{1+C_x\left(\frac{\omega_{E\times B}}{\gamma_{ITG}}\right)^2} \times \frac{1}{\max(1,(s-0.5)^2)} \quad (10)$$

where, C_x is the coefficient for each species (C_i=1.42×10^2, C_e=1.42×10^2, C_H=1.85, and C_z=1.72), s is the magnetic shear. γ_{ITG} is an approximation of linear ion temperature gradient (ITG) growth rate, estimated as v_{ti}/R , in which v_{ti} is the ion thermal velocity, $\omega_{\mathrm{E\times B}}$ is the flow shearing rate that is calculated using Equation 11:

$$\omega_{ExB} = \left| \frac{RB_\theta^2}{B_\varphi} \frac{\partial\left(E_r/RB_\theta\right)}{\partial\psi} \right| \quad (11)$$

where, ψ is the poloidal flux, and the radial electric field (E_r) can be calculated using Equation 12:

$$E_r = \frac{1}{Zen_i}\frac{\partial p_i}{\partial r} - v_\theta B_\phi + v_\phi B_\theta \quad (12)$$

where, $\partial P_i/\partial r$ is the pressure gradient, v_θ and v_ϕ are the poloidal and toroidal velocities, respectively, n_{i} is the ion density, Z is the ion charge number and e is the elementary charge. The toroidal velocity is assumed to be zero. Note that the poloidal velocity is estimated using the NCLASS module [12]. The suppression of ion thermal diffusivity (χ_{i_s}), suppression of electron thermal diffusivity (χ_{e_s}), suppression of hydrogenic particle diffusivity (D_{H_s}) and suppression of impurity particle diffusivity (D_{z_s}) are given by Equations 13-16.

$$\chi_{i_s} = \chi_i \times f_{s_{ion}} \quad (13)$$

$$\chi_{e_s} = \chi_e \times f_{s_{eletron}} \quad (14)$$

$$\mathrm{D_{H_s}} = \mathrm{D_H} \times \mathrm{f_{s_{Hydrgenic}}} \quad (15)$$

$$D_{z_s} = D_z \times f_{s_{impurity}} \quad (16)$$

2. Results and Discussion

In this work, the simulations are carried out for 10 DIII-D *H*-mode discharges using the BALDUR integrated predictive modeling code. These discharges are taken from the International Profile Database [13]. Table 1 summarizes the parameters for each discharge.

Table 1. Summary of plasma parameters for 10 DIII-D *H*-mode discharges at the diagnostic time.

Parameters	*Discharges*									
	77557	77559	81321	81329	81499	81507	82205	82788	82188	82183
R (m)	1.68	1.69	1.69	1.70	1.69	1.61	1.69	1.68	1.69	1.69
a (m)	0.62	0.62	0.60	0.59	0.63	0.54	0.63	0.62	0.63	0.54
κ	1.85	1.84	1.83	1.83	1.68	1.95	1.71	1.67	1.65	1.91
δ	0.33	0.35	0.29	0.36	0.32	0.29	0.37	0.35	0.29	0.22
B_ϕ (T)	1.99	1.99	1.98	1.94	1.91	1.91	1.87	0.94	1.57	1.57
I_p (MA)	1.00	1.00	1.00	1.00	1.35	1.34	1.34	0.66	1.33	1.33
$\bar{n}_e(10^{19}\mathrm{m}^{-3})$	4.88	5.02	2.94	5.35	4.81	4.90	5.34	2.86	6.47	6.87
Z_{eff}	1.68	2.21	2.42	1.65	2.33	1.93	2.13	1.94	1.95	1.95
P_{NB} (MW)	4.78	13.23	3.49	8.34	5.74	5.71	5.68	3.25	3.92	3.92
Time(s)	2.70	2.70	3.90	3.80	4.00	3.80	3.66	3.54	3.78	3.78

The simulation results show that the predicted plasma profiles are higher than the experimental profiles due to the over-prediction of the top of the pedestal. The example profiles of electron temperature, ion temperature, electron density, and ion density of DIII-D discharge number 81329 are shown in Figure 2.

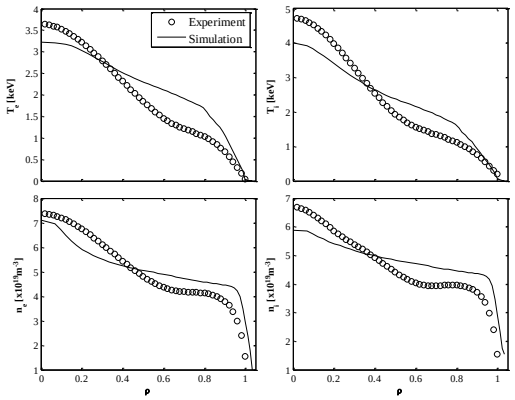

Figure 2. The profiles of electron temperature (T_e), ion temperature (T_i), electron density (n_e), and ion density (n_i) as a function of normalized minor radius. The simulation results are carried out by BALDUR code and compared to the DIII-D discharge 81329 at the diagnostic time.

Thus, to quantify the comparison between the simulation results and experimental results, the RMSE and offsets are computed using Equations 17–18:

$$\mathrm{RMSE}(\%) = \sqrt{\frac{1}{N}\sum_{i=1}^{N}\left(\frac{X_{\mathrm{sim}_i} - X_{\mathrm{exp}_i}}{X_{\mathrm{exp}_0}}\right)^2} \times 100 \qquad (17)$$

$$\mathrm{offset}(\%) = \frac{1}{N}\sum_{i=1}^{N}\left(\frac{X_{\mathrm{sim}_i} - X_{\mathrm{exp}_i}}{X_{\mathrm{exp}_0}}\right) \times 100 \qquad (18)$$

where, X_{exp_i} is the i^{th} data point of the experiment profile, X_{sim_i} is the corresponding data point of the simulation profile, and X_{exp_0} is the maximum data point of the experiment profile of X as a function of radius, which has N total number of data points. It should be noted that when the offset is positive, it indicates that the simulated profile is systematically higher than the experimental profile and negative if the simulated profile is systematically lower than the experimental

profile. Thus, in Figure 3 and 4, the RMSE of the electron temperature ranges from 10.8% to 29.6% in which the average value is 16.9%. In the case of ion temperature, the RMSE ranges from 9.3% to 28.8% and the average RMSE is 18.4%. In the case of electron density, the RMSE ranges from 9.0% to 14.1% and the average value of RMS is 11.7%; moreover, the RMSE value of ion density ranges from 12.0% to 38.4% and the average RMSE is 23.1%. Also, the offsets of four parameters are mostly positive, indicating that simulation over-predicts the experimental data.

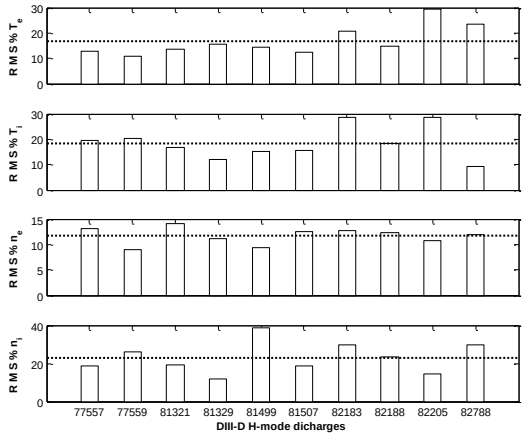

Figure 3. The RMSE% for electron temperature, ion temperature, electron density, and ion density produced by simulation of BALDUR code, compared with experimental data for 10 *H*-mode discharges by DIII-D device and the average of RMSE% in each profile is shown by dash line in each graph.

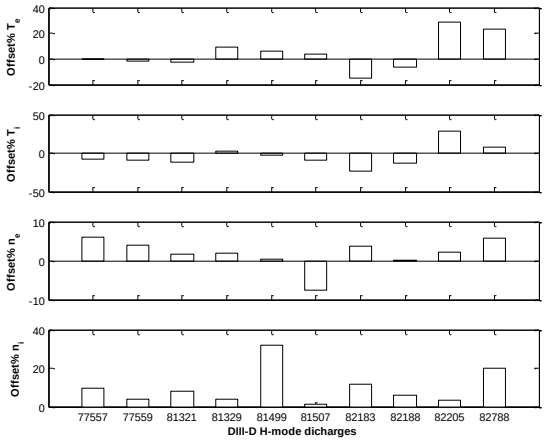

Figure 4. The offset% for electron temperature, ion temperature, electron density, and ion density produced by simulation of BALDUR code, compared with experimental data for 10 *H*-mode discharges by DIII-D device.

3. Conclusions

The complete Core-Edge-SOL model has been implemented to the integrated predictive modeling code BALDUR. The simulation results carried out by BALDUR code were validated to the experimental results of 10 *H*-mode DIII-D discharges. The average RMSE of electron temperature, ion temperature, electron density, and ion density are 16.9%, 18.4%, 11.7%, and 23.1%, respectively. However, the simulations over-predict the experiment, so the coefficient for each species C_x must be re-calibrated.

4. References

[1] Aymar, R., Barabaschi, P., and Shimonura, Y., The ITER Design, Plasma Physics and Controlled Fusion, Vol.44, No.5, pp. 519-566, 2002.

[2] Pianroj, Y., and Onjun, T., Core-SOL Simulation of L-mode Tokamak Plasma Discharges Using BALDUR Code, Songklanakarin Journal of Science and Technology, Vol. 36, No. 2, pp. 217-225, 2014.

[3] Connor, J. W., Fukuda, T., Garbet, X., Gormezano, C., Mukhovatov, V., and

Wakatani, M., A Review of Internal Transport Barrier Physics for Steady-State Operation of Tokamaks, Nuclear Fusion, Vol. 44, No. 4, pp. R1-R49, 2004.

[4] Langer, W. D., and Singer, C. E., Two-Chamber Model for Diverters with Plasma Recycling, IEEE Transactions on Plasma Science, Vol.13, No.3, pp. 163-166, 1985.

[5] Onjun, T., and Pianroj, Y., Simulations of ITER with Combined Effects of Internal and Edge Transport Barriers, Nuclear Fusion, Vol. 49, No. 7, pp.1-11, 2009.

[6] Doyle, E. J., Houlberg, W. A., Kamada, Y., Mukhovatov, V., Osborne, T. H., Polevoi, A., Bateman, G., Connor, J. W., Cordey, J. G., Fujita, T., Garbet, X., Hahm, T. S., Horton, L. D., Hubbard, A. E., Imbeaux, F., Jenko, F., Kinsey, J. E., Kishimoto, Y., Li, J., Luce, T. C., Martin, Y., Ossipenko, M., Parail, V., Peeters, A., Rhodes, T. L., Rice, J. E., Roach, C. M., Rozhansky, V., Ryter, F., Saibene, G., Sartori, R., Sips, A. C. C., Snipes, J. A., Sugihara, M., Synakowski, E. J., Takenaga, H., Takizuka, T., Thomsen, K., Wade, M. R., and Wilson, H. R., Chapter 2: Plasma Confinement and Transport, Nuclear Fusion, Vol. 47, No. 6, pp. S18-S127, 2007.

[7] Sugihara, M., Igitkhanov, Y., Janeschitz, G., and Pacher, G., Simulation Studies on *H*-mode Pedestal Behavioru During Type-I ELMs under Various Plasma Conditions, Proceedings of the 28th EPS Conference on Controlled Fusion and Plasma Physics, Funchal, Portugal, 18-22 June, 2001, pp. 629-632.

[8] Zolotukhin, O. V., Igitkhanov, Y., Janeschitz, G., and Pacher, G., Transport Simulations of Type I ELMs, Proceedings of the 28th EPS Conference on Controlled Fusion and Plasma Physics, Funchal, Portugal, 18-22 June 2001, pp. 677-680.

[9] Pankin, A. Y., Voitsekhovitch, I., Bateman, G., Dnestrovski, A., Janeschitz, G., Murakami, M., Osborne, T., Kritz, A. H., Onjun, T., Pacher, G. W., and Pacher, H. D., Combined Model for the H-mode Pedestal and ELMs, Plasma Physics and Controlled Fusion, Vol. 47, No. 3, pp. 483-504, 2005.

[10] Janeschitz, G., Pacher, G. W., Zolotukhin, O., Pereverzev, G., Pacher, H. D., Igitkhanov, Y., Strohmeyer, G., and Sugihara, M., A 1-D Predictive Model for Energy and Particle Transport in H-mode, Plasma Physics and Controlled Fusion, Vol. 44, No. 5A, pp. A459-A572, 2002.

[11] Pacher, G. W., Pacher, H. D., Janeschitz, G., Kukushkin, A. S., and Pereverzev, G., Operating Window of ITER from Consistent Core–pedestal–SOL Modelling with Modified MMM Transport and Carbon, Plasma Physics and Controlled Fusion, Vol. 46, No. 5A, pp. A257-A264, 2004.

[12] Houlberg, W. A., Shaing, K. C., Hirshman, S. P., and Zarnstorff, M. C., Bootstrap Current and Neoclassical Transport in Tokamaks of Arbitrary Collisionality and Aspect Ratio, Physics of Plasmas, Vol. 4, No. 9, pp. 3230-3242, 1997.

[13] Boucher, D., Connor, J. W., Houllberg, W. A., Turner, M. F., and Bracco, G., The International Multi-Tokamak Profile Database, Nuclear Fusion, Vol. 40, No. 12, pp. 1955-1982, 2000.